

This is the peer reviewed version of the following article:

Superposition principle for the tensionless contact of a beam resting on a winkler or a pasternak foundation / Nobili, Andrea. - In: JOURNAL OF ENGINEERING MECHANICS. - ISSN 0733-9399. - STAMPA. - 139:10(2013), pp. 1470-1478. [10.1061/(ASCE)EM.1943-7889.0000555]

Terms of use:

The terms and conditions for the reuse of this version of the manuscript are specified in the publishing policy. For all terms of use and more information see the publisher's website.

11/01/2026 20:18

(Article begins on next page)

SUPERPOSITION PRINCIPLE FOR THE TENSIONLESS CONTACT OF A BEAM RESTING ON A WINKLER OR A PASTERNAK FOUNDATION

by Andrea Nobili¹

ABSTRACT

A Green function based approach is presented to address the nonlinear tensionless contact problem for beams resting on either a Winkler or a Pasternak two-parameter elastic foundation. Unlike the traditional solution procedure, this approach allows determining the contact locus position independently from the deflection curves. In so doing, a general nonlinear connection between the loading and the contact locus is found which enlightens the specific features of the loading that affect the position of the contact locus. It is then possible to build load classes sharing the property that their application leads to the same contact locus. Within such load classes, the problem is linear and a superposition principle holds. Several applications of the method are presented, including symmetric and non-symmetric contact layouts, which can be hardly tackled within the traditional solution procedure. Whenever possible, results are compared with the existing literature.

Keywords: Tensionless contact, Green function, two-parameter elastic foundation

INTRODUCTION

The contact problem for beams resting on elastic foundations has long attracted considerable attention, given its relevance in describing soil-structure interaction (Hetenyi 1946; Selvadurai 1979). In particular, a very extensive literature exists concerning beams resting on one, two and three-parameter elastic foundations (Kerr 1964). The existing literature is for the most part devoted to considering contact as a bilateral constraint, which fact limits the validity of the analysis to situations where lift-off plays a minor role. However, in so doing, the problem retains a valuable linear character and the superposition principle holds.

¹Dipartimento di Ingegneria Meccanica e Civile, Università degli Studi di Modena e Reggio Emilia, via Vignolese 905, 41122 Modena, Italy. E-mail:andrea.nobili@unimore.it

24 When lift-off becomes an important feature, tensionless contact must be reverted to at the
25 expense of the problem linearity. From a mathematical standpoint, tensionless contact determines
26 a free-boundary problem (Kerr 1976; Nobili 2012).

27 Historically, interest in tensionless contact between a beam and a foundation arose in connec-
28 tion with railway systems. In this respect, Weitsman (1971), Lin and Adams (1987) and recently
29 Chen and Chen (2011) considered detachment and stability for the problem of tensionless contact
30 under a moving load. Besides, much research on tensionless structure-foundation contact is de-
31 voted to assessing its role in reducing the structural stress in a seismic event (Celep and Güler 1991;
32 Psycharis 2008). Recently, Coskun (2003) studied forced harmonic vibrations of a finite beam sup-
33 ported by a tensionless Pasternak soil, while Zhang and Murphy (2004) studied a finite beam in
34 tensionless contact in a non-symmetric contact scenario. Tensionless contact for an infinite beam
35 in a multiple contact scenario was investigated by Ma et al. (2009a) and Ma et al. (2009b). An
36 extensive body of literature exists regarding numerical strategies specifically devised to deal with
37 tensionless contact. Recently, Sapountzakis and Kampitsis (2010) considered a boundary element
38 method for beam-columns partly supported on a Winkler and, later (2011), a three-constant soil
39 model.

40 The classic approach to solving a tensionless contact problem for a beam on an elastic founda-
41 tion consists of integrating the deflection curves for the beam in contact, the beam in lift-off and
42 the soil, and then matching the solutions at the yet unknown contact locus, that is the point where
43 contact ceases and lift-off begins (Weitsman 1970; Kerr and Coffin 1991). This approach suffers
44 from two major shortcomings. On the one hand, the procedure initially assumes a contact layout
45 and then proceeds to determining the relevant quantities within such layout. It then remains to be
46 checked that results are consistent with the assumptions. On the other hand, contact loci positions
47 are determined through deflection curves integration. Since the general integrals of the governing
48 equations depend on the loading, it appears that results are restricted to one particular loading.

49 In this paper, a Green function approach is adopted. Unlike the classic approach, this method
50 consists of first determining the contact locus through a nonlinear equation and then solving the

51 linear problem for the deflection curves. In fact, only the first stage is here presented, the second
 52 being a classic problem. Although the method still requires some assumptions concerning the lay-
 53 out of the contact, nonetheless such assumptions are somewhat relaxed and a general connection
 54 between the contact locus and a family of loadings is obtained, so much so that a form of superposi-
 55 tion is also retrieved. It is emphasized that this procedure differs from the integral approach of Tsai
 56 and Westmann (1967), which is still based on the Green function and yet it aims at determining the
 57 deflection curves and the contact locus in one stage.

58 THE FREE-BOUNDARY PROBLEM

59 The tensionless contact problem for a Euler–Bernoulli (E-B) beam resting on a tensionless
 60 elastic foundation is first stated in its simplest form, concerning a Winkler soil in a symmetric
 61 contact scenario (Fig.1). Let $[-X, X]$ denote the contact interval and $X > 0$ be the *contact locus*,
 62 i.e. the beam rests supported on the soil up to abscissa X and then it detaches from it. The beam
 63 detached from the soil is often addressed as lifting off the soil. The free soil extends beyond
 64 X to infinity. Here, the inverse of a reference length is introduced as the ratio between the soil
 65 modulus k and the beam flexural rigidity EI , i.e. $\beta^4 = k(4EI)^{-1}$. Then, the problem is cast in
 66 dimensionless form: $\Xi = \beta X$ is the dimensionless contact locus position and $u = \beta w$ denotes the
 67 beam dimensionless displacement. The beam displacement function, u , restricted to the contact
 68 interval $I^c = [0, \Xi]$ and to the lift-off interval $I^l = (\Xi, l]$, is denoted by u^c and u^l , respectively.
 69 $2l = 2\beta L$ is the beam dimensionless length and u^s is the soil dimensionless displacement in
 70 the unbounded region $I^s = [\Xi, +\infty)$, which is relevant for the Pasternak soil alone. Besides,
 71 $\sigma^c = \beta q^c/k$ and $\sigma^l = \beta q^l/k$ are the dimensionless loadings acting in I^c and I^l , respectively. In the
 72 contact interval I^c , the beam rests entirely supported on the soil and the governing equation reads

$$\frac{1}{4} (u^c)^{(iv)} + u^c = \sigma^c, \quad (1)$$

73 where superscripts within parenthesis denote the differentiation order with respect to ξ . To shorten
 74 notation, it is expedient to write the k -th derivative $(u^c)^{(k)}$ with respect to ξ as u_k^c . The problem

75 boundary conditions (BCs) due to symmetry are

$$u_1^c(0) = 0, \quad u_3^c(0) = 0, \quad (2)$$

76 while the BCs at the contact locus Ξ , enforce continuity for the beam of the bending moment and
77 of the shearing force

$$u_2^c(\Xi) = u_2^l(\Xi), \quad u_3^c(\Xi) = u_3^l(\Xi). \quad (3)$$

78 However, unlike an ordinary boundary value problem (BVP), here the contact locus is a problem
79 unknown, whence a further condition is demanded for its placing. This condition, named *con-*
80 *tact locus equation*, enforces displacement continuity with the Winkler foundation (which is here
81 assumed load free), i.e.

$$u^c(\Xi) = 0. \quad (4)$$

82 In more general terms, the problem may be rewritten formally as

$$D^c u^c = \sigma^c \quad (5)$$

83 where D^c denotes the differential operator embodying the dimensionless governing equation in the
84 contact region I^c , with its boundary conditions.

85 THE GREEN FUNCTION APPROACH

86 In this paper, a new solution procedure is introduced which takes advantage of the Green func-
87 tion to obtain an explicit connection between the loading and the contact locus position. Let the
88 adjoint problem for Eq.(5) be considered

$$\tilde{D}^c G(\xi, \zeta) = \delta(\xi, \zeta), \quad (6)$$

89 where $\delta(\xi, \zeta)$ is Dirac's delta function about $\xi = \zeta$ and \tilde{D}^c the adjoint operator. Let n indicate the
90 order of the operator D^c , i.e. $n = 4$ for both the Pasternak and the Winkler models. It is worth

91 recalling that the Green function G is determined assuming homogeneous boundary conditions at
 92 the boundary ∂I^c and it is thereby independent of the behavior in the lift-off region. The latter
 93 comes into play in the form of a boundary term $BT(\xi, \zeta)$. Furthermore, a over-determined system
 94 becomes an under-determined problem for the Green function. It is then possible to write the
 95 displacement at a point ζ in the contact region as

$$u^c(\zeta) = \int_{I^c} \sigma^c(\xi)G(\xi, \zeta)d\xi \quad (7)$$

96 and, accordingly, the condition setting the contact locus. For instance, for a Winkler foundation, it
 97 is

$$u^c(\Xi) = \lim_{\zeta \rightarrow \Xi} \int_{I^c} \sigma^c(\xi)G(\xi, \zeta)d\xi - [BT(\xi, \Xi)]_{\xi=0}^{\Xi} = 0. \quad (8)$$

98 Here, boundary terms are algebraic and have been gathered in $BT(\xi, \Xi)$. Eq.(8) sets an integral
 99 connection between the applied loading and the contact locus Ξ which has a three-fold purpose.
 100 First, it may be employed to test a given load distribution against the contact locus Ξ . Second, it
 101 may be employed to build the loading classes $\mathcal{Q}_{\mathcal{X}}$, whose elements share the property that their
 102 application produces the same set of contact loci $\mathcal{X} = \{\Xi_j\}$. Then, the nonlinear contact problem
 103 of a beam resting on a tensionless two-parameters elastic soil may be actually solved for any one
 104 representative of the load class, the solution for the other load members of that class being obtained
 105 by linear combination. The third purpose of the condition is to provide the contact locus without
 106 recurring to the actual integration of the deflection curves.

107 TENSIONLESS WINKLER-TYPE SOIL

108 Let us first consider the case of a E-B beam resting on a tensionless Winkler soil and acted upon
 109 by a line load σ^c (the resultant of which is indeed irrelevant owing to the homogeneous nature of
 110 the BC setting the contact locus) possibly extending up to (though vanishing at) the contact locus
 111 Ξ , in a symmetric continuous contact scenario. Here, the BCs (3) are homogeneous. The boundary
 112 term reads

$$BT = \frac{1}{4} [u_3^c G - u_2^c G' + u_1^c G'' - u^c G''']_0^{\Xi}. \quad (9)$$

113 Here, prime denotes differentiation with respect to ξ , while G is shorthand for $G(\xi, \zeta)$. It is easily
 114 seen that to warrant the vanishing of the boundary term, the Green function has to be subjected to
 115 symmetric conditions at $\xi = 0$

$$G'(0, \zeta) = G'''(0, \zeta) = 0 \quad (10)$$

116 and to the single condition

$$G'''(\Xi, \zeta) = 0. \quad (11)$$

117 such that the beam slope $u_1^c(\Xi)$ drops out the boundary term. This result holds in general, even
 118 when the loading extends beyond the contact locus, which amounts to saying that the Green func-
 119 tion is entirely independent of the lift-off part. The problem for the Green function is under-
 120 determined and it possesses one free integration parameter.

121 The ODE for the Green function is

$$\frac{1}{4}G^{(iv)}(\xi, \zeta) + G(\xi, \zeta) = \delta(\xi, \zeta), \quad (12)$$

122 whose general solution is written as

$$G(\xi, \zeta) = \left\{ \begin{array}{l} a_i(\zeta, \Xi), \quad \xi < \zeta \\ b_i(\zeta, \Xi), \quad \xi > \zeta \end{array} \right\} \eta_i(\xi), \quad i = 1, \dots, n. \quad (13)$$

123 Here, $\{\eta_i(\xi)\}$ is the fundamental set and, for a Winkler soil,

$$\{\eta_i(\xi)\} = \{e^\xi \cos \xi, e^\xi \sin \xi, e^{-\xi} \cos \xi, e^{-\xi} \sin \xi\}. \quad (14)$$

124 Hereinafter, a summation convention is assumed for twice repeated subscripts, ranging from 1 to
 125 n . Let us further enforce the BC

$$G'''(\Xi, \zeta) = 0, \quad (15)$$

126 whence a self-adjoint formulation for G is set. Since the problem is self adjoint, the Green function

127 is symmetric as it allows exchanging the role of ξ and ζ . Through Eq.(13), the contact zone
 128 displacement is given by

$$u^c(\zeta) = a_i(\zeta, \Xi) \int_0^\zeta \sigma^c(\xi) \eta_i(\xi) d\xi + b_i(\zeta, \Xi) \int_\zeta^\Xi \sigma^c(\xi) \eta_i(\xi) d\xi, \quad \zeta \in [0, \Xi]. \quad (16)$$

129 In particular, letting $\zeta \rightarrow \Xi$, it is $u^c(\zeta) \rightarrow 0$ according to Eq.(4). Letting

$$F(\Xi) = \alpha_i(\Xi) A_i(\Xi), \quad (17)$$

130 where

$$A_i(\Xi) = a_i(\Xi, \Xi), \quad \alpha_i(\Xi) = \int_0^\Xi \sigma^c(\xi) \eta_i(\xi) d\xi, \quad (18)$$

131 it is $F(\Xi) = 0$. It is remarked that Eqs.(18) should be taken in a limiting sense as $\zeta \rightarrow \Xi$,
 132 although direct substitution is equally permitted for the Winkler foundation. In particular, explicit
 133 expressions are available for the functions A_i , namely

$$A_1 = A_3 = 2\Lambda^{-2} \cos(\Xi) \cosh(\Xi), \quad (19a)$$

$$A_2 = -A_4 = 2\Lambda^{-2} \sin(\Xi) \sinh(\Xi), \quad (19b)$$

134 having let the nonnegative quantity $\Lambda^2 = \sin(2\Xi) + \sinh(2\Xi)$. Eq.(17), with Eqs.(14) and (19),
 135 may be rewritten as

$$F(\Xi) = \alpha_+(\Xi) \cos(\Xi) \cosh(\Xi) + \alpha_-(\Xi) \sin(\Xi) \sinh(\Xi), \quad (20)$$

136 where $2\alpha_+(\Xi) = \alpha_2(\Xi) + \alpha_4(\Xi)$, $2\alpha_-(\Xi) = \alpha_1(\Xi) - \alpha_3(\Xi)$. The dependence from the loading is
 137 completely embedded in the functions $\alpha_+(\Xi)$, $\alpha_-(\Xi)$ and it is clear that different loadings giving
 138 the same functions are equivalent inasmuch as the contact locus is concerned. Eq.(20) acquires a
 139 particularly simple form when it exists $\rho^c < \Xi$ such that the loading vanishes outside the interval

140 $[0, \rho^c]$, for then

$$\tan(\Xi) \tanh(\Xi) = -\frac{\alpha_+(\rho^c)}{\alpha_-(\rho^c)} = r \quad (21)$$

141 and the RHS r is a constant with respect to Ξ . It is observed that for r positive the contact locus
 142 sits in the interval $(\pi/2, \pi)$ and, by solution continuity, for r negative in $(\pi, \frac{3}{2}\pi)$. In this situation,
 143 loadings are equivalent inasmuch as they exhibit the same ratio r . For instance, in the case of
 144 two symmetric pairs of concentrated forces, placed at Δ_1 and $\Delta_2 > \Delta_1$, it is

$$r = -\frac{\cos(\Delta_1) \cosh(\Delta_1) + \cos(\Delta_2) \cosh(\Delta_2)}{\sin(\Delta_1) \sinh(\Delta_1) + \sin(\Delta_2) \sinh(\Delta_2)} \quad (22)$$

145 such that solving the implicit equation $r = k$, k being a real constant, gives the set of pairs Δ_1, Δ_2
 146 yielding the same contact locus $\Xi(k)$. Fig.2 shows the curves $\Delta_2 - \Delta_1$ vs. Δ_1 for $k = 1, 5, 10$.
 147 The curves may be taken as a graphical representation of the sets \mathcal{Q}_k . Indeed, Fig.3 shows that
 148 for $k = 1$, the deformed beam profiles for the cases $\Delta_2 - \Delta_1 = 0.1$ and $\Delta_2 - \Delta_1 = 1$, to which
 149 it pertains respectively $\Delta_1 = 0.8857167949$ and $\Delta_1 = 0.2529526456$, exhibit the same contact
 150 locus position $\Xi(1) = 2.347045566$. Among such loadings the superposition principle does hold.
 151 Eq.(20) is generally nonlinear in Ξ owing to both the functions α_i and A_i .

152 Let us now investigate the contribution of the boundary term and consider the situation where
 153 the beam is loaded beyond the contact locus through the line load $\sigma^l(\xi), \Xi < \xi < l$. Then, a
 154 boundary term enters the function F . Exploiting the symmetry of the Green function and the
 155 continuity of its first derivative, Eq.(17) becomes

$$F(\Xi) = \left\{ \alpha_i(\Xi) - \frac{1}{4}u_3^s(\Xi)\eta_i(\Xi) + \frac{1}{4}u_2^s(\Xi)\eta_i'(\Xi) \right\} A_i(\Xi) \quad (23)$$

156 where, in analogy with the first of Eqs.(18), it is let $B_i(\Xi) = b_i(\Xi, \Xi)$. With a bit of work, Eq.(20)

157 is now

$$\alpha_+(\Xi) \cos(\Xi) \cosh(\Xi) + \alpha_-(\Xi) \sin(\Xi) \sinh(\Xi) = \frac{1}{8} u_3^c(\Xi) [\cosh(2\Xi) + \cos(2\Xi)] - \frac{1}{8} u_2^c(\Xi) [\sinh(2\Xi) - \sin(2\Xi)]. \quad (24)$$

158 Eq.(24) provides a nonlinear equation relating the loading and the contact locus, in a symmetric
 159 layout, which gathers all the nonlinear feature of the unilateral contact problem. It also provides a
 160 mean of determining whether the beam lifts off the foundation or, rather, rests entirely supported
 161 on it. To this aim, solutions of Eq.(24) are checked against the beam length l and when it is found
 162 that $\Xi > l$, then the beam rests entirely supported by the foundation.

163 **Applications for a Winkler soil**

164 *Symmetric case*

165 Let us consider the case of a beam loaded at midspan by a unit force. Then, it is $\alpha_+ = 1$,
 166 $\alpha_- = 0$ and Eq.(20) reduces to the simple relation

$$\cosh \Xi \cos \Xi = 0, \quad (25)$$

167 which corresponds to Eq.(7) of Weitsman (1970) and yields the well-known result $\Xi = \pi/2$. We
 168 are interested in adding an end force f^l and an end couple c^l such that the contact locus remains
 169 unchanged. To this aim, a relationship between $u_2^c(\Xi)$ and $u_3^c(\Xi)$ needs be sought in order that the
 170 boundary contribution drops out. Writing the latter as at the RHS of Eq.(24) and considering that

$$\frac{1}{4} u_2^c(\Xi) = c^l + f^l(l - \Xi), \quad \frac{1}{4} u_3^c(\Xi) = -f^l, \quad (26)$$

171 given that f^l is positive when downwards and c^l when clockwise, a connection is found between
 172 c^l and f^l as follows:

$$c^l = -f^l (l - \Xi + R^W(\Xi)), \quad (27)$$

173 where the positive function is let

$$R^W(\Xi) = \frac{\cosh(2\Xi) + \cos(2\Xi)}{\sinh(2\Xi) - \sin(2\Xi)}. \quad (28)$$

174 In particular, for $\Xi = \pi/2$, it is $R^W(\Xi) = 0.6536439910$.

175 As a second application, the case of a pair of concentrated forces, symmetric about $\xi = 0$ and
 176 placed at a distance $2\Delta > 0$ apart, is considered. Then, it is $\alpha_i = \eta_i(\Delta)$ and Eq.(21) gives a
 177 connection between the contact locus and the distance $\Delta < \Xi$, namely

$$\tan \Xi \tanh \Xi = -\frac{1}{\tan \Delta \tanh \Delta}. \quad (29)$$

178 It is immediate to see that the sign of both the left and the right hand side is given by the tangent
 179 terms: for $\Delta \in [0, \pi/2)$, the RHS is negative and solutions are to be found in the interval $\Xi \in$
 180 $[\pi/2, \pi)$. By the same token, for $\Delta \in [\pi/2, \pi)$, continuity of the solution suggests taking $\Xi \in$
 181 $[\pi, \frac{3}{2}\pi)$. It is further observed that the situation $\Delta = \Xi$ is not allowed. If the applied forces are far
 182 apart beyond a limiting spacing $2\tilde{\Delta}$, lift-off takes place in the neighborhood of the origin as well,
 183 in a discontinuous contact scenario. Such limiting spacing occurs when

$$u^c(0) = b_i(0, \Xi) \int_0^\Xi \sigma^c(\xi) \eta_i(\xi) d\xi = b_i(0, \Xi) \eta_i(\tilde{\Delta}) = 0 \quad (30)$$

184 and the grazing condition $u_1^c(0) = 0$ follows directly from the symmetry requirement. Here, it is

$$b_1(0, \Xi) = \frac{1}{2\Lambda^2} [\cos(2\Xi) + \cosh(2\Xi) - \sinh(2\Xi) - \sin(2\Xi) + 2]$$

$$b_2(0, \Xi) = \frac{1}{2\Lambda^2} [\cos(2\Xi) - \cosh(2\Xi) + \sinh(2\Xi) + \sin(2\Xi)]$$

185 and $b_2(0, \Xi) + b_4(0, \Xi) = 1$, $b_1(0, \Xi) - b_3(0, \Xi) = -1$. For a general Δ , Eq.(30) with Eq.(29)
 186 yields

$$b_2(0, \Xi) - b_1(0, \Xi) \tan \Xi \tanh \Xi = f(\Delta), \quad (31)$$

187 being

$$f(\Delta) = -\frac{e^{-\Delta}}{2 \sinh \Delta} (1 + \cot \Delta). \quad (32)$$

188 Eq.(31) lends a connection between the contact locus and the spacing Δ . Since $\Delta > 0$ demands
 189 $\Xi > \pi/2$, the LHS of (31) is positive and to get a positive value for the RHS it must be $\Delta > \tilde{\Delta} =$
 190 2.356194490. Fig.4 shows the beam bending moment, shearing force and contact pressure in the
 191 contact interval. As on the verge of lifting-off, the latter vanishes at midspan.

192 As a third example, Eq.(24) is put to advantage for the case of a constant line loading q extend-
 193 ing up to the abscissa l_q and a concentrated force $2f_0$ at midspan. When $l_q = l$ the classic solution
 194 for a concentrated load $2f_0$ acting at midspan of a beam with weight per unit length q is obtained.
 195 This situation is generally more involved than the previous ones because, for l_q large enough, the
 196 contact locus sits within the loaded interval. Eq.(24) gives

$$2f_0 \cos \Xi \cosh \Xi + \frac{q}{2} [\sinh 2\Xi + \sin 2\Xi] = -q(l_q - \Xi) [\cosh 2\Xi + \cos 2\Xi] \\ - \frac{1}{2}q(l_q - \Xi)^2 [\sinh 2\Xi - \sin 2\Xi], \quad (33)$$

197 provided that $l_q > \Xi$. When $l_q < \Xi$ it is

$$2f_0 \cos \Xi \cosh \Xi + q [\cos l_q \sinh l_q + \sin l_q \cosh l_q] \cos \Xi \cosh \Xi \\ + q [-\cos l_q \sinh l_q + \sin l_q \cosh l_q] \sin \Xi \sinh \Xi = 0. \quad (34)$$

198 For $f_0 = 1$, Fig.5 plots both Eqs.(33,34) in their realms of validity, the boundary between them
 199 being represented by the bisector. It is seen that for q small ($q = 0.01$), the contact locus tends to
 200 the classic result $\pi/2$ in a wide range of l_q . At $q = 0.05$, it is observed that for a given l_q multiples
 201 solutions for Ξ are found and a maximum value for $l_q > \Xi$ appears. Beyond such maximum, a
 202 second branch of solution exists with $\Xi > l_q$. It rests to be seen whether the beam is long enough
 203 to warrant the admissibility of such solution. In order to discuss the multiplicity of solutions, Fig.6
 204 shows the beam profiles for $q = 0.05$ and $l_q = 3$, when the solution $\Xi < l_q$, curve (a), and $\Xi > l_q$,

205 curve (b), are considered. It is seen that the solution (b) leads to interpenetration and must be
 206 discarded. However, above the maximum value for l_q , solution (a) disappears and solution (b)
 207 becomes admissible.

208 *Non-symmetric case*

209 Let us now drop the symmetry assumption and deal with a general continuous contact scenario
 210 (Fig.7). Then, two contact loci, $\Xi_1 < \Xi_2$, are expected and Eq.(16) becomes

$$u^c(\zeta) = a_i(\zeta, \Xi_1, \Xi_2) \int_{\Xi_1}^{\zeta} \sigma^c(\xi) \eta_i(\xi) d\xi + b_i(\zeta, \Xi_1, \Xi_2) \int_{\zeta}^{\Xi_2} \sigma^c(\xi) \eta_i(\xi) d\xi. \quad (35)$$

211 Likewise, two limits are now considered

$$\lim_{\zeta \rightarrow \Xi_2} u^c(\zeta) = 0 \quad \Leftrightarrow \quad \alpha_i(\Xi_1, \Xi_2) A_i(\Xi_1, \Xi_2) = 0, \quad (36a)$$

212

$$\lim_{\zeta \rightarrow \Xi_1} u^c(\zeta) = 0 \quad \Leftrightarrow \quad \alpha_i(\Xi_1, \Xi_2) B_i(\Xi_1, \Xi_2) = 0, \quad (36b)$$

213 having let $A_i(\Xi_1, \Xi_2) = a_i(\Xi_2, \Xi_1, \Xi_2)$, $B_i(\Xi_1, \Xi_2) = b_i(\Xi_1, \Xi_1, \Xi_2)$ and $\alpha_i = \int_{\Xi_1}^{\Xi_2} \sigma^c(\xi) \eta_i(\xi) d\xi$.

214 Despite the fact that the analysis follows along the same path as in the symmetric situation, the
 215 increased mathematical complication suggests to limit the discussion to a single concentrated force.

216 Then, $\sigma^c = \delta(\xi, \Delta)$ and it is expedient to set the ξ -axis origin at $\xi = \Delta$ without loss of generality.

217 Eqs.(36) become

$$A_1(\Xi_1^*, \Xi_2^*) + A_3(\Xi_1^*, \Xi_2^*) = 0, \quad (37a)$$

$$B_1(\Xi_1^*, \Xi_2^*) + B_3(\Xi_1^*, \Xi_2^*) = 0, \quad (37b)$$

218 with the understanding that $\Xi_1^* = \Xi_1 - \Delta$ and likewise $\Xi_2^* = \Xi_2 - \Delta$. It is easy to show that for a
 219 symmetric disposition of the contact loci, i.e. $\Xi_1^* = -\Xi_2^*$, Eqs.(37) collapse into a single equation,
 220 which corresponds to Eq.(25). Indeed, every time a solution exists with $\Xi_1^* = -\Xi_2^*$ for either of
 221 the Eqs.(37), then it complies with both. It is natural to introduce $d = \Xi_1^* + \Xi_2^*$, the deviation

222 with respect to a symmetric condition (Fig.7). Fig.8 draws the solution curves d vs. Ξ_2^* for the
223 first (dash curve) and the second (solid curve) of Eqs.(37). In this plot, each intersection point
224 is a possible solution of the system. The shaded area, bounded from below by the dotted curve
225 $d = 2\Xi_2^*$, is ruled out as it leads to a contact locus $\Xi_1^* > \Xi_2^*$. It is seen that a discrete number
226 of solutions is available yet the ones with minimum Ξ_2^* and d are specially interesting. As long
227 as $l_2 \geq \Delta + \pi/2$, which means that the solution points at $\Xi_2^* \geq \pi/2$ are admissible, the classic
228 solution $d = 0$, corresponding to a symmetric layout, is retrieved (point A in Fig.8). When such
229 condition no longer holds, one of the beam ends plunges into the foundation, say the right end,
230 whence it is $\Xi_2 = l_2$ fixed. Then, only the second equation of (37) survives (solid curve) and it
231 provides d vs. $\Xi_2^* = l_2 - \Delta$. Note that $\Xi_1^* = d - \Xi_2^*$ or, equivalently, $\Xi_1 = d - l_2 + 2\Delta$.

232 It is interesting to describe the system behavior as Δ increases and the loading is brought closer
233 and closer to the beam end. Then, d is found moving along the solid curve from point A to point
234 B and beyond, until the origin is reached. It is seen that d acquires decreasing (with Δ) negative
235 values until the point B is reached, where the layout with maximum deviation from symmetry $|d|$
236 is found. Since, for the most part, the solid curve possesses unit slope, in the neighborhood of A it
237 is $d \approx -\Delta$ and the left contact locus moves rightwards proportionally with Δ , i.e. $\Xi_1 \approx -l_2 + \Delta$.
238 The contact imprint, however, is given by $l_c = \Xi_2 - \Xi_1$ and it shrinks as

$$l_c \approx 2l_2 - \Delta. \quad (38)$$

239 Fig.9 plots the position of the left contact locus against the loading offset Δ for a beam with
240 $l_2 = \pi/2$, that is starting from point A . Since both the absolute position Ξ_1 and the relative
241 position Ξ_1^* are given, the difference between the curves equals Δ , while the distance $l_2 - \Xi_1$ gives
242 the contact imprint length l_c . The deviation from symmetry, d , is also shown as the difference
243 from the dash-dot curve and $-l_2$. Dotted curves show the positive and negative unit slope, which
244 confirm the behavior previously inferred for Ξ_1, l_c and d . Beyond B , a substantial rotation of the
245 beam occurs which leads to a very small contact imprint and an almost symmetric situation. Here,

246 d increases towards zero again.

247 It is easy to obtain the results numerically developed in Zhang and Murphy (2004) for a beam
248 of varying length l loaded symmetrically and non-symmetrically by a unit force. Three regimes
249 are considered:

- 250 1. when $\Xi_2 < l_2$ and $|\Xi_1| < l_1$,
- 251 2. when, say, $\Xi_2 > l_2$ and $|\Xi_1| < l_1$,
- 252 3. when $\Xi_2 > l_2$ and $|\Xi_1| > l_1$.

253 In regime 1, both left and right contact loci sit inside the beam, the symmetric solution $d = 0$ is
254 admitted and the contact imprint length $l_c = \Xi_2 - \Xi_1 = 2\Xi_2^*$ is constant. In regime 2, the beam right
255 length l_2 is too short to warrant that the right contact locus sits inside the beam. Conversely, the
256 left length l_1 accommodates the left contact locus. It is observed that this regime demands a non-
257 symmetric loading situation. Having let $l_2 = k_2 l$ and $\Delta = k_\Delta l$, where $k_2, k_\Delta < 1$, Eq.(38) shows
258 that the contact imprint length scales linearly with l with a proportionality coefficient $2k_2 - k_\Delta$.
259 Finally, regime 3 is such that both contact loci exceed the beam left and right length. The beam
260 rests entirely supported by the soil and the contact imprint length corresponds to the beam length.
261 In a symmetric layout, beam length scaling brings the system from regime 1 to regime 3 or vice
262 versa and the contact imprint length is either constant or equal to l , as numerically found in Zhang
263 and Murphy (2004). In a non-symmetric layout, the system undergoes all three regimes and, from
264 1 to 3, the contact imprint length is constant, decreases with coefficient $2k_2 - k_\Delta$ and finally equals
265 the beam length, i.e. coefficient 1.

266 PASTERNAK SOIL

267 Let us consider the case of a E-B beam resting on a tensionless Pasternak soil in a symmetric
268 continuous contact scenario. The governing ODE reads, in the contact interval,

$$\frac{1}{4}u_4^c - \alpha u_2^c + u^c = \sigma^c, \quad (39)$$

269 where the dimensionless quantity $\alpha = \beta^2 k_G/k$ is introduced and k_G is the shear modulus of the
 270 foundation (Selvadurai 1979). The BCs enforce symmetry at $\xi = 0$, as at Eqs.(2), and bending
 271 moment and shearing force continuity at the contact locus Ξ , as in (3). Furthermore, two BCs
 272 involve the soil profile through setting displacement and slope continuity (Kerr 1976), i.e.

$$u^c(\Xi) = u^s(\Xi), \quad u_1^c(\Xi) = u_1^s(\Xi). \quad (40)$$

273 The problem is only formally self-adjoint, as the Green function for the beam in the contact region
 274 is determined by symmetric BCs at $\xi = 0$, as at Eqs.(10), and homogeneous conditions at $\xi = \Xi$
 275 as follows:

$$\frac{1}{4}G''(\Xi, \zeta) - \alpha G(\Xi, \zeta) = 0, \quad \frac{1}{4}G'''(\Xi, \zeta) - \alpha G'(\Xi, \zeta) = 0. \quad (41)$$

276 It is observed that, in the limit for $\alpha \rightarrow 0$, the BCs (11,15) for the Winkler soil are retrieved. The
 277 displacement in the contact region at $\zeta < \Xi$ is given by

$$u^c(\zeta) = \int_0^\Xi \sigma^c(\xi)G(\xi, \zeta)d\xi - \frac{1}{4}[u_3^c G - u_2^c G']_0^\Xi + \left[\left(-\frac{1}{4}G''' + \alpha G \right) u_1^c + \left(\frac{1}{4}G'''' - \alpha G'' \right) u^c \right]_0^\Xi, \quad (42)$$

278 where $G(\xi, \zeta)$ takes the shape (13) and, of course, the functions $a_i(\zeta, \Xi)$ and $b_i(\zeta, \Xi)$ differ from
 279 the case of the Winkler foundation. The fundamental set is taken in even/odd fashion

$$\{\eta_i(\xi)\} = \left\{ \cosh\left(\sqrt{\lambda_1}\xi\right), \sinh\left(\sqrt{\lambda_1}\xi\right), \cosh\left(\sqrt{\lambda_2}\xi\right), \sinh\left(\sqrt{\lambda_2}\xi\right) \right\}.$$

280 Here, for the sake of definiteness, it is assumed $\alpha > 1$ whence $\lambda_{1,2} = 2\left(\alpha \pm \sqrt{\alpha^2 - 1}\right)$. The term
 281 in square brackets at RHS of (42) vanishes owing to the BCs (2,10,41).

282 In the absence of a soil loading σ^s , it is $u_1^s = -\alpha^{-1/2}u^s$, whence the BCs (40) yield the contact
 283 locus equation

$$u^c(\Xi) + \sqrt{\alpha}u_1^c(\Xi) = 0. \quad (43)$$

284 Eq.(43) sets the contact locus without recurring to the soil profile. It may be written as

$$F(\Xi) = \int_0^\Xi \sigma^c(\xi)K(\xi, \Xi)d\xi - \frac{1}{4} \lim_{\zeta \rightarrow \Xi} [u_3^c K(\Xi, \zeta) - u_2^c K'(\Xi, \zeta)], \quad (44)$$

285 wherein a new kernel function is defined in terms of the Green function G

$$K(\xi, \zeta) = G(\xi, \zeta) + \sqrt{\alpha} \frac{\partial G}{\partial \zeta}(\xi, \zeta). \quad (45)$$

286 Now the argument runs parallel to the treatment given for the Winkler soil. However, it is empha-
 287 sized that neither the kernel G nor K is symmetric, for the problem for the Green function is no
 288 longer self-adjoint. When the beam lifting-off the soil is load-free, Eq.(44) gives an expression
 289 formally analogous to (17)

$$F(\Xi) = \mathcal{A}_i(\Xi)\alpha_i(\Xi), \quad (46)$$

290 being understood that $\mathcal{A}_i(\Xi) = A_i(\Xi) + \sqrt{\alpha}\bar{A}_i(\Xi)$ and

$$A_i(\Xi) = \lim_{\zeta \rightarrow \Xi} a_i(\zeta, \Xi), \quad \bar{A}_i(\Xi) = \lim_{\zeta \rightarrow \Xi} \frac{\partial a_i}{\partial \zeta}(\zeta, \Xi). \quad (47)$$

291 The symmetric layout accounts for the vanishing of the functions A_2, A_4 and likewise for \bar{A}_2, \bar{A}_4 .
 292 Besides, A_1 equals A_3 and \bar{A}_1 equals \bar{A}_3 provided that the role of λ_1 and λ_2 is exchanged. After
 293 some lengthy manipulations, it is found, omitting a common non-vanishing denominator,

$$\mathcal{A}_1 = \lambda_1(\lambda_1 - \lambda_2) \left[\cosh(\sqrt{\lambda_2}\Xi) + \sqrt{\alpha\lambda_2} \sinh(\sqrt{\lambda_2}\Xi) \right], \quad (48a)$$

$$\mathcal{A}_3 = \lambda_2(\lambda_2 - \lambda_1) \left[\cosh(\sqrt{\lambda_1}\Xi) + \sqrt{\alpha\lambda_1} \sinh(\sqrt{\lambda_1}\Xi) \right], \quad (48b)$$

294 whence A_1 and A_3 are easily retrieved letting $\alpha \rightarrow 0$. As expected, \mathcal{A}_3 equals \mathcal{A}_1 once the role of
 295 λ_1 and λ_2 is exchanged.

296 When accounting for the contribution from the lift-off interval, it is

$$F(\Xi) = \mathcal{A}_i(\Xi)\alpha_i(\Xi) - \frac{1}{4} [u_3^c(\Xi)\mathcal{A}_i(\Xi)\eta_i(\Xi) - u_2^c(\Xi)\mathcal{A}_i(\Xi)\eta_i'(\Xi)], \quad (49)$$

297 where use has been made of the continuity properties of the Green function G .

298 **Applications for a Pasternak soil**

299 Let us consider the classic situation of a beam resting on a tensionless Pasternak soil and
 300 loaded at midspan by a unit force. Then, it is $\sigma^c = \delta(\xi, 0)/2$ and Eq.(46), together with Eqs.(48)
 301 and divided through by $(\lambda_1 - \lambda_2)$, gives

$$F(\Xi) = \lambda_1 \left[\cosh\left(\sqrt{\lambda_2}\Xi\right) + \sqrt{\alpha\lambda_2} \sinh\left(\sqrt{\lambda_2}\Xi\right) \right] \\ - \lambda_2 \left[\cosh\left(\sqrt{\lambda_1}\Xi\right) + \sqrt{\alpha\lambda_1} \sinh\left(\sqrt{\lambda_1}\Xi\right) \right]. \quad (50)$$

302 The first positive root of F gives, when $\beta = 2.5$, the result $\Xi = 0.8423946552$. We wish to
 303 determine the loading condition at the beam end such that the contact locus is preserved. Again,
 304 we need to vanquish the last term of Eq.(49), i.e.

$$c^l = f^l (l - \Xi + R^P(\Xi)), \quad R^P(\Xi) = \frac{\mathcal{A}_i(\Xi)\eta_i(\Xi)}{\mathcal{A}_i(\Xi)\eta_i'(\Xi)}.$$

305 It is observed that for $\alpha \rightarrow 0$ the Pasternak soil becomes a Winkler soil and indeed $R^P(\Xi) \rightarrow$
 306 $R^W(\Xi)$. In particular, for $\Xi = 0.8423946570$, it is $R^P(\Xi) = 0.2763085352$.

307 When two symmetrically placed unit forces are far apart enough, the beam stands on the verge
 308 of lifting off at the origin. Letting the force distance be 2Δ and making use of Eqs.(48), Eq.(46)
 309 specializes to

$$F(\Xi) = \lambda_1 \cosh(\sqrt{\lambda_1}\Delta) \left[\cosh\left(\sqrt{\lambda_2}\Xi\right) + \sqrt{\alpha\lambda_2} \sinh\left(\sqrt{\lambda_2}\Xi\right) \right] \\ - \lambda_2 \cosh(\sqrt{\lambda_2}\Delta) \left[\cosh\left(\sqrt{\lambda_1}\Xi\right) + \sqrt{\alpha\lambda_1} \sinh\left(\sqrt{\lambda_1}\Xi\right) \right], \quad (51)$$

310 having omitted the common factor $\lambda_1 - \lambda_2$ and provided that $\alpha > 1$. Seeking the solution of
 311 $F(\Xi) = 0$ lends the curves Ξ vs. Δ . For a Pasternak foundation, the counterpart of Eq.(30)
 312 demands that the dimensionless contact pressure $-u_4^c/4$ vanishes at the origin. With Eq.(39), the
 313 requirement amounts to

$$\alpha_i(\Xi) \left(B_i(\Xi) - \alpha \bar{\bar{B}}_i(\Xi) \right) = 0, \quad (52)$$

314 being, in analogy with Eq.(47), $B_i(\Xi) = \lim_{\zeta \rightarrow \Xi} b_i(\zeta, \Xi)$, $\bar{\bar{B}}_i(\Xi) = \lim_{\zeta \rightarrow \Xi} \frac{\partial^2 b_i}{\partial \zeta^2}(\zeta, \Xi)$. Fig.10 plots
 315 the solution curves of Eq.(51) (dash) and Eq.(52) (solid curve) for $\alpha = 1.1, 5$ and 10 . The bisector
 316 is also plotted as a dotted line for solutions are admissible inasmuch as $\Xi > \Delta$. When the forces are
 317 brought farther apart, the contact locus position moves along the dash curve until the solid curve
 318 is met. At such limiting distance $2\tilde{\Delta}$, the continuous contact scenario breaks down and lift-off
 319 appears in the neighborhood of the origin.

320 CONCLUSIONS

321 In this paper, the free-boundary problem of tensionless contact for a beam resting on either
 322 a Winkler or a Pasternak two-parameter elastic foundation is addressed. The classic approach to
 323 the problem consists of integrating the deflection curves for the beam in contact with the soil, the
 324 beam lifting off it and the soil and then matching solutions at the contact locus, which is a problem
 325 unknown. When matching solutions, an extra condition exists that determines the contact locus.
 326 Conversely, in this paper, a Green function approach is put forward which aims at determining a
 327 direct (nonlinear) connection between the loading and the contact locus. Once the contact locus is
 328 set, the problem reduces to solving a classic linear BVP in the contact and lift-off regions. This
 329 way of approaching the problem lends considerable advantages over the classic one. First, the
 330 connection between the contact locus position and the loading is expressed as a general relation,
 331 which allows to determine what features of the loading affect the contact locus. This implies
 332 that it is possible to build the set of loadings whose application leads to the same contact locus.
 333 Among such loadings, the superposition principle holds. Second, solutions are obtained once some
 334 assumptions are made concerning the contact layout. Accordingly, results must be checked against

335 such assumptions at the end of the procedure. Although this part is common to both approaches, it
336 is shown that here the required assumptions are weaker. For instance, the non-symmetric contact
337 problem for a Winkler foundation is analyzed in general and two families of solution curves are
338 obtained: one for the left and one for the right contact locus. When the beam length is insufficient
339 to accommodate both contact loci, one curve is simply dropped in place of the constraint that
340 fixes the contact at the beam end. Conversely, when deflection curves are integrated, whether
341 lift-off exists needs be assumed from the start, given that the BCs depend on such assumption.
342 Several applications are presented for both the cases of symmetric and non-symmetric contact.
343 Furthermore, comparison with the existing literature is carried out.

344 REFERENCES

- 345 Celep, Z. and Güler, K. (1991). “Dynamic response of a column with foundation uplift.” *J. Sound*
346 *Vib.*, 149(2), 285 – 296.
- 347 Chen, J.-S. and Chen, Y.-K. (2011). “Steady state and stability of a beam on a damped tensionless
348 foundation under a moving load.” *Int. J. Non Linear Mech.*, 46(1), 180 – 185.
- 349 Coskun, I. (2003). “The response of a finite beam on a tensionless Pasternak foundation subjected
350 to a harmonic load.” *Eur. J. Mech. A. Solids*, 22(1), 151 – 161.
- 351 Hetenyi, M. (1946). *Beams on elastic foundations*. Ann arbor: the university of Michigan press.
- 352 Kerr, A. D. (1964). “Elastic and viscoelastic foundation models.” *J. Appl. Mech.*, 31(3), 491–498.
- 353 Kerr, A. D. (1976). “On the derivation of well posed boundary value problems in structural me-
354 chanics.” *Int. J. Solids Struct.*, 12(1), 1–11.
- 355 Kerr, A. D. and Coffin, D. W. (1991). “Beams on a two-dimensional Pasternak base subjected to
356 loads that cause lift-off.” *Int. J. Solids Struct.*, 28(4), 413 – 422.
- 357 Lin, L. and Adams, G. G. (1987). “Beam on tensionless elastic foundation.” *J. Eng. Mech.*, 113(4),
358 542–553.
- 359 Ma, X., Butterworth, J., and Clifton, G. (2009a). “Response of an infinite beam resting on a ten-
360 sionless elastic foundation subjected to arbitrarily complex transverse loads.” *Mech. Res. Com-*
361 *mun.*, 36(7), 818–825.

362 Ma, X., Butterworth, J., and Clifton, G. (2009b). "Static analysis of an infinite beam resting on a
363 tensionless Pasternak foundation." *Eur. J. Mech. A. Solids*, 28(4), 697-703.

364 Nobili, A. (2012). "Variational approach to beams resting on two-parameter tensionless elastic
365 foundations." *J. Appl. Mech.* To appear.

366 Psycharis, I. N. (2008). "Investigation of the dynamic response of rigid footings on tensionless
367 Winkler foundation." *Soil Dyn. Earthquake Eng.*, 28(7), 577 – 591.

368 Sapountzakis, E. and Kampitsis, A. (2010). "Nonlinear dynamic analysis of timoshenko beam-
369 columns partially supported on tensionless Winkler foundation." *Comput. Struct.*, 88(21,22),
370 1206 – 1219.

371 Sapountzakis, E. J. and Kampitsis, A. E. (2011). "Nonlinear analysis of shear deformable beam-
372 columns partially supported on tensionless three-parameter foundation." *Arch. Appl. Mech.*,
373 81(12), 1833–1851.

374 Selvadurai, A. P. S. (1979). *Elastic analysis of soil-foundation interaction*, Vol. 17 of *Developments*
375 *in geotechnical engineering*. Elsevier scientific publishing company, Amsterdam - Oxford - New
376 York.

377 Tsai, N. and Westmann, R. (1967). "Beam on tensionless foundation." *J. Eng. Mech.*, 93(EM5),
378 1–12. Proc. Paper 5495.

379 Weitsman, Y. (1970). "On foundations that react in compression only." *J. Appl. Mech.*, 37(4),
380 1019–1030.

381 Weitsman, Y. (1971). "Onset of separation between a beam and a tensionless elastic foundation
382 under a moving load." *Int. J. Mech. Sci.*, 13(8), 707 – 711.

383 Zhang, Y. and Murphy, K. D. (2004). "Response of a finite beam in contact with a tensionless
384 foundation under symmetric and asymmetric loading." *Int. J. Solids Struct.*, 41(24,25), 6745 –
385 6758.

386 **List of Figures**

387 1 Symmetric continuous contact scenario with lift-off for a beam on a tensionless
388 Winkler foundation 22

389 2 $\Delta_1, \Delta_2 - \Delta_1$ pairs giving the same contact locus $\Xi(k)$ 23

390 3 Beam profile for $k = 1$ and either $\Delta_2 - \Delta_1 = 1$ or $\Delta_2 - \Delta_1 = 0.1$ 24

391 4 Bending moment, shearing force and contact pressure for a beam on a Winkler
392 foundation at the onset of midspan lift-off 25

393 5 l_q vs Ξ for $f_0 = 1$ as given by Eqs.(33,34) 26

394 6 Beam profiles for $\Xi < l_q$ (a) and $\Xi > l_q$ (b), for $q = 0.05, l_q = 3, f_0 = 1$ 27

395 7 Beam on a Winkler soil in a non-symmetric layout 28

396 8 Plots of the first (dash) and the second (solid) of Eqs.(37) 29

397 9 Left contact locus absolute (solid) and relative (dash) position for a beam loaded
398 by a concentrated force at $\xi = \Delta$ 30

399 10 Ξ vs. Δ curve (dash) for $\alpha = 1.1, 5$ and 10 , and limiting curve (solid) which marks
400 the onset of a discontinuous contact scenario 31

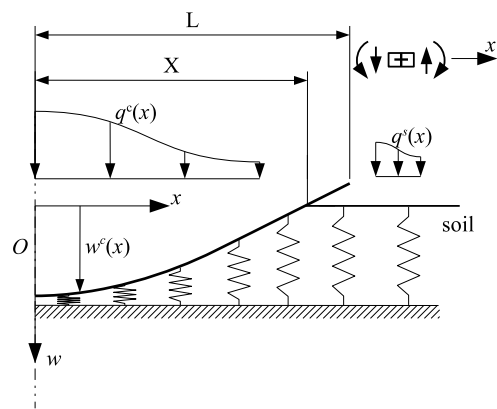


FIG. 1. Symmetric continuous contact scenario with lift-off for a beam on a tensionless Winkler foundation

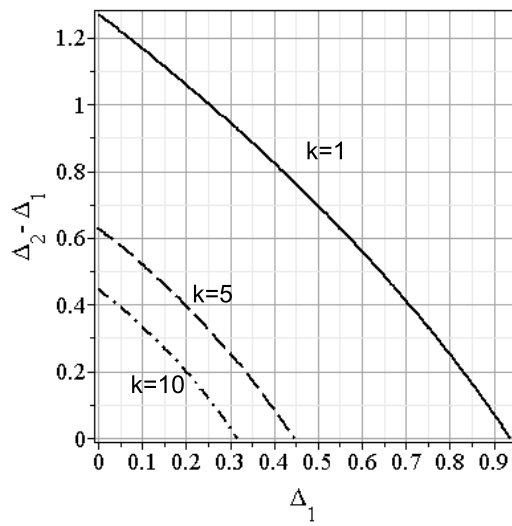


FIG. 2. $\Delta_1, \Delta_2 - \Delta_1$ pairs giving the same contact locus $\Xi(k)$

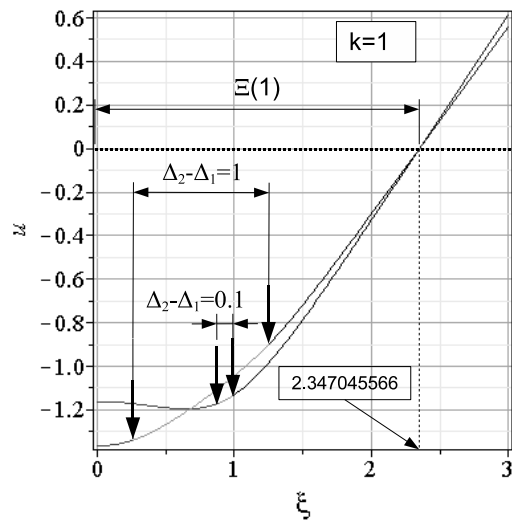


FIG. 3. Beam profile for $k = 1$ and either $\Delta_2 - \Delta_1 = 1$ or $\Delta_2 - \Delta_1 = 0.1$

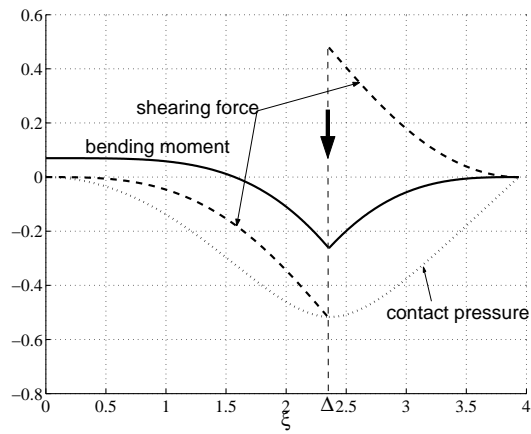


FIG. 4. Bending moment, shearing force and contact pressure for a beam on a Winkler foundation at the onset of midspan lift-off

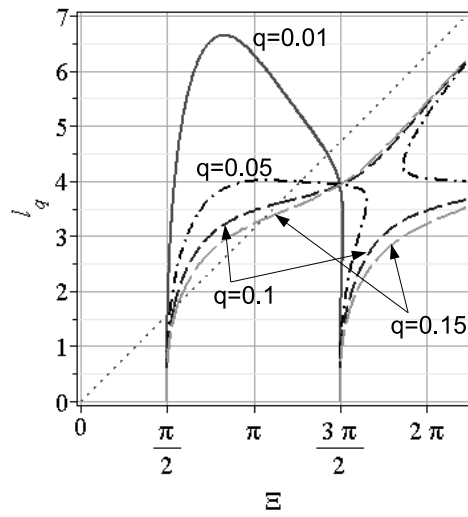


FIG. 5. l_q vs Ξ for $f_0 = 1$ as given by Eqs.(33,34)

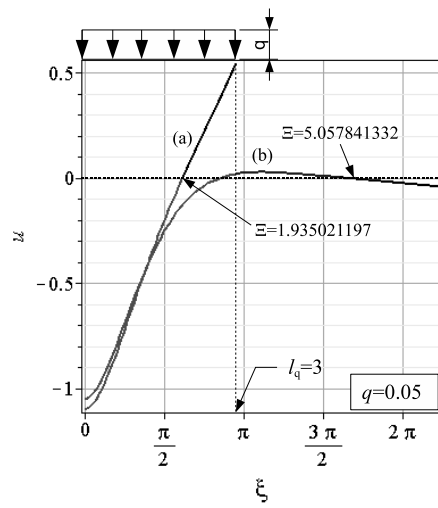


FIG. 6. Beam profiles for $\Xi < l_q$ (a) and $\Xi > l_q$ (b), for $q = 0.05, l_q = 3, f_0 = 1$

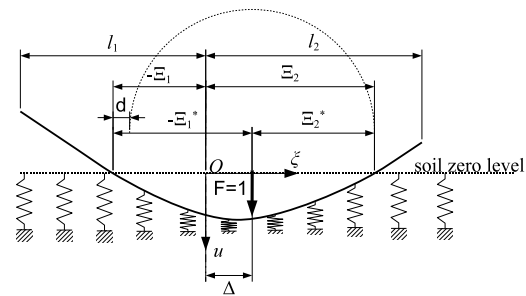


FIG. 7. Beam on a Winkler soil in a non-symmetric layout

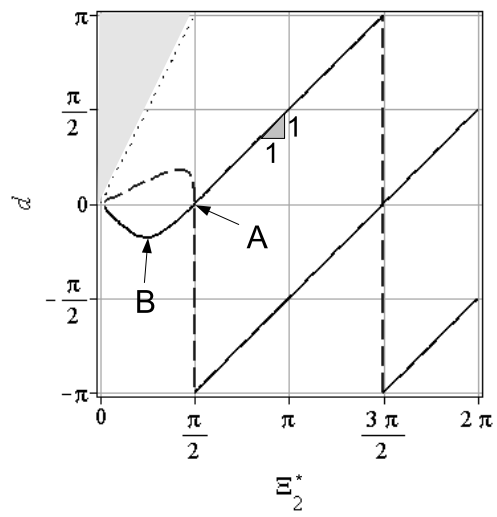


FIG. 8. Plots of the fist (dash) and the second (solid) of Eqs.(37)

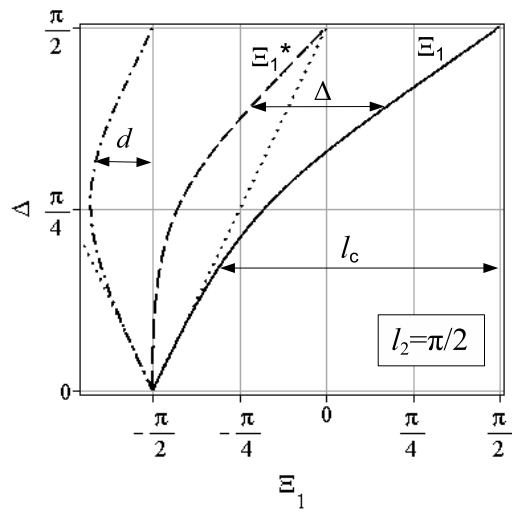


FIG. 9. Left contact locus absolute (solid) and relative (dash) position for a beam loaded by a concentrated force at $\xi = \Delta$.

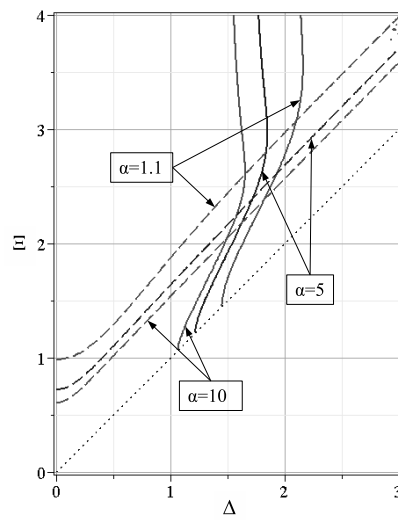


FIG. 10. Ξ vs. Δ curve (dash) for $\alpha = 1.1, 5$ and 10 , and limiting curve (solid) which marks the onset of a discontinuous contact scenario